JOURNAL OF
Optical Communications
and Networking

STAR: a carrier sense agnostic MAC scheme for a crowded NLoS-FSOC optical LAN

Paa Kwesi Esubonteng,[1,*] Hieu Pham Trung Nguyen,[2] and Roberto Rojas-Cessa[1,3]

[1]Networking Research Laboratory, Department of Electrical and Computer Engineering, New Jersey Institute of Technology, Newark, New Jersey 07102, USA
[2]Department of Electrical and Computer Engineering, Nano-Optoelectronic Materials and Devices Laboratory, New Jersey Institute of Technology, Newark, New Jersey 07102, USA
[3]e-mail: rojas@njit.edu
*Corresponding author: pae5@njit.edu

Received 10 May 2022; revised 9 August 2022; accepted 30 August 2022; published 19 September 2022

Nondirect line-of-sight free-space optical communications (NLoS-FSOC) operate based on an optical wireless broadcast channel shared by multiple stations to communicate, thus forming an optical local area network (OLAN). Such a channel in the NLoS-FSOC is generated by a diffuse reflector (DR) that reflects light equally in all directions except toward itself. While the broadcast channel of an OLAN is accessible to many stations as in radio-frequency wireless LANs, the signal strength of the reflected beam in an OLAN depends not only on the receiver-DR distance, but also on the angle of incidence of the transmitted beam. An incident beam with a wide angle generates a weak reflected signal that may be undetectable by some stations in the communication range. The loss of the reflected power may render channel sensing ineffective. To address this challenge, we propose the use of the access point to indicate the time to attempt accessing the channel. We also propose a medium access control (MAC) scheme for OLANs using explicit start rather than the conventional channel sensing. The proposed MAC scheme, called STAR, not only enables stations to contend for the available channel, but also decreases collisions, and in turn, stations experience high throughput and low delay. Furthermore, we generalize STAR for the transmission of voice, video, and data traffic. We compare STAR to leading MAC schemes, adapted for their use on an OLAN. We show that STAR achieves 83% throughput for differential traffic and is a 15% higher throughput than the throughput of IEEE 802.11.

https://doi.org/10.1364/JOCN.463602

1. INTRODUCTION

The emergence of connected autonomous vehicles and appliances demands high-data rate connectivity to the cloud [1]. Such applications may rely on heavy computation in the cloud and high-bandwidth connectivity to upload and download the sensed and processed data.

Optical wireless or free-space optical communications (FSOC) constitute a tentative communications approach for satisfying the application requirements as it provides unmatched bandwidth and data rates [2,3], privacy [4–6], and long-distance capabilities [7,8]. However, it is unlikely that FSOC will be adopted for such applications because it operates only as point-to-point links and requires direct line-of-sight (LoS) between the transmitting and receiving parties at all times.

Fortunately, such limitations can be overcome by nondirect LoS FSOC or NLoS-FSOC [9–11], which is an approach using a diffuse reflector (DR) to enable all stations with a direct LoS to the DR to share a channel. The DR is made of an inert material reflecting the incident light with equal intensity to all directions except toward its own surface. In this approach, the DR reflects the incident laser light toward the stations in the area with LoS, and it creates a broadcast optical channel. In such a channel, any station can transmit to all stations in the network, and all stations can receive a transmission, or what we call a broadcast-channel optical local area network (OLAN).

The NLoS-FSOC, like FSOC, is immune to electromagnetic interference [12,13] and can achieve high data rates. On the other hand, the broadcast channel in the NLoS-FSOC requires attention to privacy, range asymmetry, and angle of transmission incidence. Range asymmetry in the NLoS-FSOC means that a transmitter can be far away from the DR (even a few km), but the receiver must be moderately close to the DR because the power of the reflected light rapidly decreases as the distance increases. More interestingly, the angle of the incident beam with respect to the DR also affects the reflected power. As the angle of incidence increases, the power of the reflected light decreases. This means that some stations may be unable to detect a busy channel and experience a collision, despite having the transmitter and receiver in an adequate range.

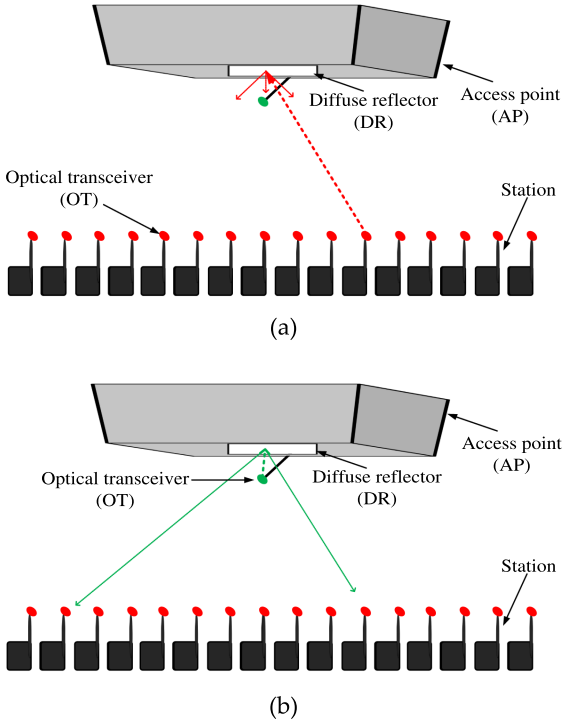

Fig. 1. Uplink and downlink transmissions in an OLAN. (a) Uplink from stations. (b) Downlink from the access point.

To allow having transmitters with a wide angle of incidence, one can place an access point (AP) in close proximity to the DR such that any transmission can be detected by it. Here, we adopt this setup as a structured network mode, where the stations communicate with the Internet or other stations through an AP, as shown in Fig. 1. In this model, an uplink (UL) transmission refers to a transmission from a station to the AP, as shown in Fig. 1(a). Likewise, the downlink (DL) is a transmission from the AP to one or multiple stations, as shown in Fig. 1(b). Here, we consider that both UL and DL transmissions are reflected on the same DR.

However, with an optical broadcast channel, the NLoS-FSOC requires a medium access control (MAC) scheme to define how the stations access the channel. We focus on this challenge in this paper. There are many MAC schemes for radio-frequency (RF) networks, such as IEEE 802.11 and many others [14–24]. But unlike RF networks, the effect of the angle of incidence on the strength of the reflected signal in NLoS-FSOC requires the design of a new MAC scheme that rescinds from channel sensing. Therefore, this feature raises the question whether a MAC scheme based on explicit start of the contention period for NLoS-FSOC can be as effective as channel sensing for a functional and effective operation in an OLAN. We address this question by proposing a MAC scheme, called the sequential slotted MAC scheme for nondirect LoS FSOC (STAR), for an NLoS-FSOC OLAN that in lieu of channel sensing resorts to the use of explicit start of the contention slot.

With an explicit start, the start time for channel contention is indicated to the stations in the OLAN, so they can contend for channel access. Moreover, to increase the network performance, we resort to station awareness so that the network is cognizant of the number of stations in the OLAN through a detection mechanism to size the contention period large enough to reduce transmission collisions and small enough to make it efficient.

We show the performance of STAR by theoretically estimating its throughput and by performing exhaustive evaluations of throughput, consumed energy, delay, and fairness and compare it to leading RF MAC schemes adapted for their use in an OLAN for multiple classes of traffic. We show that STAR not only achieves high throughput, but also outperforms the compared schemes.

In summary, the contributions of this paper are 1) the proposal of a time slot structure for OLAN-focused MAC schemes that rescinds from channel sensing as an approach to contention in a broadcast optical channel and 2) the proposal of a MAC scheme, called STAR, that uses explicit start in lieu of channel sensing. STAR uses the proximity of the AP to the DR to sense the channel and the AP to signal to the competing stations the time to attempt accessing the channel. STAR is designed to support not only best-effort traffic, but also traffic with different classes. We also theoretically formulate the throughput of STAR and confirm its correctness by showing a close correspondence to the simulated throughput. We show the performance of STAR in terms of average delay, consumed energy, and service fairness and compare it to leading MAC schemes adapted for operating in an OLAN. We show that STAR outperforms IEEE 802.11 and the compared schemes.

The remainder of this paper is organized as follows. Section 2 discusses the existing works on MAC schemes and how STAR is positioned. Section 3 introduces our proposed time slot structure and MAC scheme. Section 4 presents an analytical model for the STAR scheme. Section 5 compares the performance of the STAR to IEEE 802.11 and other similar schemes. Section 6 draws our conclusions.

2. RELATED WORK

Wireless channel access can be classified as contention- or non-contention-based. The point coordination function (PCF) is a non-contention-based medium access approach, popularly used in the IEEE 802.11 standard, where the AP polls the stations to transmit packets. IEEE 802.11 also uses a contention-based access approach, or the distributed coordination function (DCF), where stations attempt to capture the transmission channel for packet transmission after sensing it as available for packet transmission [25]. While they are not a global practice, the PCF and DCF are both adopted by many wireless MAC schemes to make use of their individual or combined characteristics.

MAC schemes that rescind from channel sensing have been considered before. Examples of those are the early ALOHA [26] and the more recent multiple access with collision avoidance by invitation (MACA-BI) [21].

In ALOHA, a station transmits its packet and waits for an acknowledgment (ACK). Its reception proves a successful transmission, but a silent period indicates otherwise. ALOHA suffers from throughput degradation for a large number of contending stations or under heavy loads [27,28]. MACA-BI uses polling instead of channel sensing, where an idle station that

is ready to receive a packet transmits a ready-to-receive (RTR) packet so that any station that has a packet for the receiver can attempt a transmission. A transmission includes information on the backlog at the transmitting station so that the receiving station may continue sending invitations in the future. MACA-BI may suffer from throughput degradation when the traffic pattern changes among the transmitting stations [21,29].

Channel-reservation MAC schemes, such as channel reservation and cooperative relay (CRCR) [30] and early backoff announcement (EBA) MAC, eliminate the need for carrier sensing by reserving slots for transmission [31]. In such schemes, a station announces to the entire network the time its next packet is transmitted, and all stations in the network become informed on future time-slot reservations. A station that has no reservation may select an available time slot for its coming transmission. While channel reservation techniques drastically reduce collision rates, they also increase transmission overhead, besides requiring additional memory to store the reservations.

Macaluso *et al*. [10] proposed the first MAC schemes for NLoS-FSOC, which is based on channel sensing. Here, a station with a packet to transmit projects a light beam onto the DR requesting access to the channel. The scheme detects a reflected beam that is free from spatial collision. This work showed space-time trade-offs may be considered in access schemes. However, the angle of incidence problem may jeopardize the scheme operation. Carrier-sense schemes are the norm in RF wireless networks. Such schemes have been widely studied, and some of them can achieve high performance. Examples of those are IEEE 802.11 [14], the quality QOS Categories Activeness-aware Adaptive EDCA (QCAAAE) [32], and more recently, the StaTion pREsence Awareness in crowded networks algorithM (STREAM) [33].

IEEE 802.11 is the standard multiple access scheme based on carrier sense. This scheme can handle multiple classes of traffic, and it has been proved over time to be very versatile. However, it is sensitive to crowding effects; the throughput of the network decreases in a crowded or loaded network.

QCAAAE is similar to IEEE 802.11, except that it is aware of the number of stations in the network. This information is used for sizing the congestion window. The AP plays a role in the estimation of this information.

STREAM is another station-presence-aware scheme in which the selection of contention periods is based on the number of stations in the network. It uses a contention period whose duration is proportional to the estimated number of stations so that collisions are reduced.

Different from the existing schemes, STAR uses explicit start of the contention period, in which stations attempt to capture the channel, and without prior sensing. STAR is also station presence aware, as it uses that to achieve high performance. Table 1 presents a summarized comparison of the discussed MAC schemes in this section. Note that QCAAAE, STREAM, and STAR are the only schemes that consider multiclass traffic and are network occupancy aware.

Table 1. Comparison of the Discussed MAC Schemes

Scheme	Principle	Performance	Multi-class Traffic	Network Occupancy Aware
CRCR	Channel	High	No	Yes
EBA	reservation		No	Yes
802.11		High	Yes	No
QCAAAE	Carrier		Yes	Yes
STREAM	sense		Yes	Yes
Macaluso			No	No
ALOHA	Carrier sense	Low	No	No
MACA-BI	agnostic		No	Yes
STAR	Explicit start	High	Yes	Yes

3. TIME SLOT STRUCTURE AND PROPOSED MAC SCHEME

A. NLoS-FSOC and Channel Sensing Problem

For clarity, we list the terms and notations used in this paper in Table 2.

In an optical channel, the received power P_{rx} can be expressed as [9]

$$P_{rx} = \frac{P_t R \cos\theta A_r}{\pi d_{rx}^2}, \tag{1}$$

where P_t is the power of the transmitted light, R is the reflectance of the DR, θ is the incidence angle between the transmitted light and the DR's normal, A_r is the aperture area of the photodiode lens at the receiver, and d_{rx} is the distance between the receiver lens and the DR. From Eq. (1), the received power is affected by R, θ, and d_{rx}, while assuming that all communicating devices have the same P_t and A_r. The selection of the DR material must consider the transmission wavelengths of the UL and DL so that $R \cong 1$. In the network, θ and d_{rx} are determined by the location of the transmitting device and the receiving lens, respectively. For instance, the ground distance d_{tx} between the transmitting station and the DR's normal affects θ, as shown in Fig. 2. The figure shows that a large d_{tx} produces a large θ and that d_{rx} varies for each receiver. More importantly, θ also affects the intensity of reflected light. Here, we consider that stations are capable of acquiring, tracking, and pointing their transceivers to the DR as they move through the coverage area.

Let ϕ be the smallest received power at which the optical channel is considered busy. Then, the channel is idle when a station senses $P_{rx} < \phi$. However, this consideration could be the product of having a transmission with a large θ so that a station with a small d_{rx} may still be unable to sense whether the channel is busy.

A simple alternative to overcome the loss of the reflected signal due to the large angle of incidence in NLoS-FSOC is using a large P_t that guarantees $P_{rx} \geq \phi$ for the largest d_{rx}, but such a high power might pose safety concerns to human and fauna eyesight, in addition to the consumption of large amounts of energy. Alternatively, the largest d_{rx} can be reduced so that P_t may be enough to sense the channel as busy; however, this approach significantly reduces the communications range and thus the area of coverage.

Table 2. Notations Used in This Paper

Notation	Description	Association
σ	Minimum duration of a contention slot	Network
PIFS	Time interval for which channel is considered idle	Network
SIFS	Time interval between frame transmissions	Network
RTS	Packet indicating a station's intent to transmit data	Station
CTS	Packet indicating station is cleared to transmit data	AP
ACK	Acknowledgment packet	AP
VO	Voice packet	Station
VI	Video packet	Station
DA	Data packet	Station
SP	Start packet	AP
NSP	New slot packet	AP
CW_e	Explicit contention window	Station
X	Segment of CW_e	Station
BO	Backoff value	Station
a	Number of contention attempts of a station	Station
n	Number of stations	Network
N	Number of packets	Network
a_{VO}	Number of contentions allowed in CW_e for VO traffic	Station
a_{VI}	Number of contentions allowed in CW_e for VI traffic	Station
a_{DA}	Number of connections allowed in CW_e for DA traffic	Station
t_σ	Duration of a σ	AP
t_{PIFS}	Duration of a PIFS	Network
t_{SIFS}	Duration of an SIFS	Network
t_{ACK}	Duration of an ACK	AP
t_{CTS}	Duration of a CTS	AP
t_{RTS}	Duration of an RTS	Station
t_{VO}	Duration of VO packet	Station
t_{VI}	Duration of VI packet	Station
t_{DA}	Duration of DA packet	Station
t_{SP}	Duration of an SP	AP
t_{NSP}	Duration of an NSP	AP

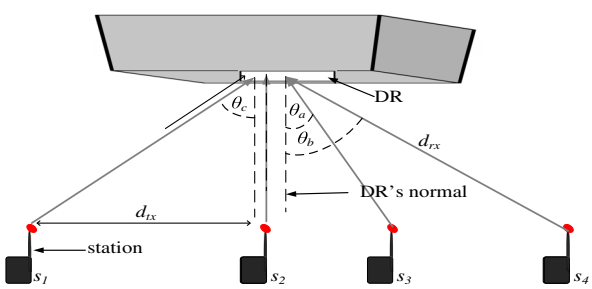

Fig. 2. Impact of d_{tx} on θ.

Therefore, we resort to the placement of an AP in the very near proximity to the DR so that it can effectively sense the channel state (i.e., a fixed and small d_{rx}). This approach allows the AP to inform the competing stations within the range of its transmissions of an idle channel. Thus, the uplink transmission can be sent at large distances from the DR. However, the size of the coverage area is determined by the largest d_{rx} at which a station receives downlink transmissions from the AP. Nevertheless, this feature of a NLoS-FSOC OLAN also calls for revisiting the use of channel sensing by stations in the network, which is popularly used in MAC schemes for RF networks.

B. Example of NLoS-FSOC in a Laboratory Experiment

Figure 3(a) shows a signal projected on the DR and detected by the receiver. This is an example of how the light may be projected and detected by the stations with a LoS to the DR. The light from the transmitter is modulated and projected onto the DR using continuous wave modulation (CWM). The reflected beam from the DR falls on the receiver, a DET100A2 silicon photodetector, whose analog output is connected to a Siglent 2304X oscilloscope and waveform generator. DET100A2 has a sensitivity $(\rho) \cong 0.65$ A/W at 852 nm, $A_r = 75.2$ mm^2, and can detect a CWM up to 10 MHz.

The voltage from the generated waveform is added in series to that of a Rigol DP831A programmable power supply providing a constant current and voltage to the transmitter diode so that the intensity of the light from the laser diode is varied according to the voltage of the generated waveform. This allows the CWM of the transmitter's light onto the DR, as shown in Fig. 3(b) where a sine wave (yellow wave) is modulated to show CWM in NLoS-FSOC. The green wave in the figure is the received waveform from the receiver. The frequency of the generated wave in the experiment is 10 MHz, and the time difference between the peaks of the generated and received wave is 80 ns. The received signal shows how the reflected signal carries the information (wave) transmitted by the incident laser light.

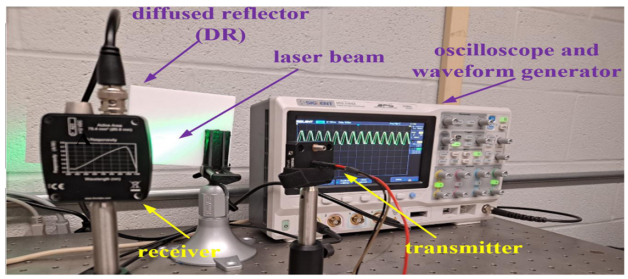

(a)

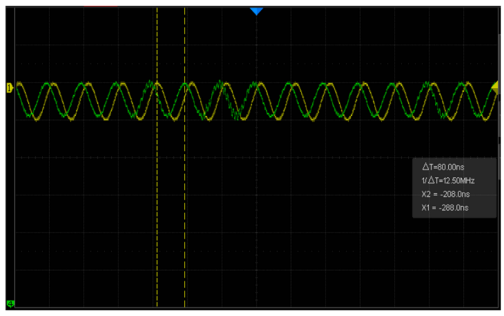

(b)

Fig. 3. Transmitted and received signal. (a) Continuous wave modulation setup. (b) Graph of modulated and demodulated sine waves.

C. Proposed Time Slot Structure

In STAR, the AP not only is the intermediate gateway for all transmissions from the stations in the network but also indicates the time when the channel is available for access. It announces the beginning of a new cycle and the contention slots by transmitting a start packet (SP) to indicate the start of the explicit congestion window (CW_e), which is a set of contention slots. A new slot packet (NSP) indicates the start of a contention slot as shown in Fig. 4(a). A cycle is the number of time slots where each slot is designated for contention. The number of contention slots in the cycle depends on the number of stations in the network and the classes of service. In each contention slot, stations are allowed to contend for channel access. Therefore, the transmissions from the AP, by design, are detectable by the stations in the area of coverage. A successful channel access occurs if only one station contends, and a collision occurs if two or more stations contend during the contention slot. Time slots 1–3 in Fig. 4(a) show an idle, unsuccessful and successful capture of the optical channel, respectively.

The SP packet carries the CW_e size, as a number of contiguous contention slots, and a list of the allowed number of contention attempts a in CW_e for each traffic class c. The classes of traffic are prioritized by having voice (VO) as the top priority, video (VI) as the medium priority, and data (DA) as the lowest priority. The CW_e size changes according to the experienced network performance, represented as collision, successful packet transmission, or an idle time slot. Here, a is adjusted for the next CW_e by the AP to improve network performance.

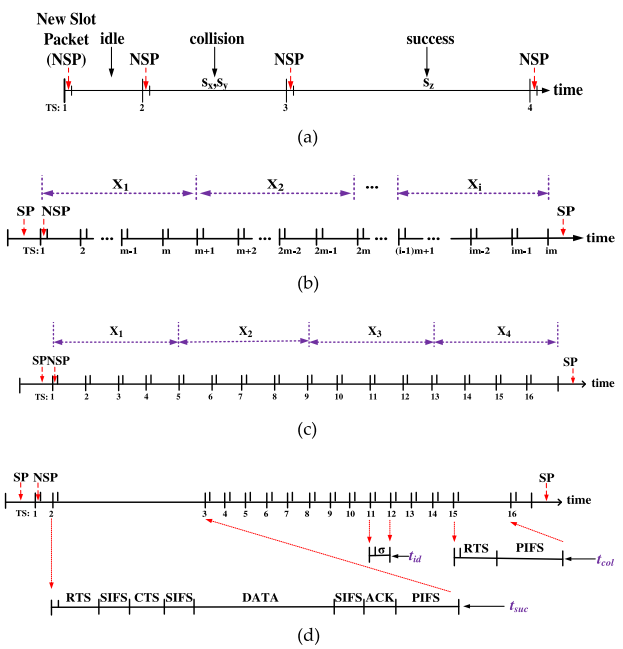

Fig. 4. Proposed time slot structure, CW_e, X, and the constituent of events in a time slot for STAR. (a) Proposed time slot structure for an optical channel. (b) Explicit contention window, CW_e, and its segments and contention slots. (c) Example of four segments X in a $\mathrm{CW}_e = 16$. (d) Constituents of successful, idle, and failed contention in a time slot.

A station that aims to compete for channel access listens and waits for the SP. The station divides the CW_e size by a to obtain the length of what we call a segment. A segment (X) is the number of contiguous time slots in which the station is allowed to contend for the channel only once. Figure 4(b) shows a CW_e and Xs in STAR, and Fig. 4(c) shows an example of Xs for video traffic with $\{\mathrm{CW}_e, a_{\mathrm{VO}}, a_{\mathrm{VI}}, a_{\mathrm{DA}}\} = \{16, 4, 2, 1\}$, where a_{VO}, a_{VI}, and a_{DA} are the number of contention attempts for VO, VI, and DA packets, respectively. The size of each segment is calculated as

$$X_i = \left[\frac{i-1}{a}\mathrm{CW}_e + 1 : \frac{i}{a}\mathrm{CW}_e\right], \tag{2}$$

where X_i is the ith segment in the CW_e. The number of backoff (BO) time slots for the station in X_i is randomly chosen as

$$\mathrm{BO} = \mathrm{random}[X_i] - \psi, \tag{3}$$

where ψ is the current time slot. STAR may adjust a as the time passes to find an appropriate number of transmission opportunities according to the priority of the traffic classes and the existing access demand per traffic class.

D. Proposed STAR Scheme

STAR uses the proposed slot structure to indicate when stations can contend for channel access, and a version of contention avoidance, as that in IEEE 802.11. In addition, it adjusts the CW_e size to accommodate for the load of the different traffic classes.

STAR starts with the transmission of the SP and the first NSP. If a station has a packet to transmit, it sets the BO in the current segment X_i after the SP is received, and it decreases it by 1 after receiving each NSP until the BO reaches 0, at which point the station contends for the channel. Contention in STAR follows the four-way handshake model of the DCF, where a station transmits a request-to-send (RTS) to the AP at the beginning of a contention slot. The AP transmits a clear-to-send (CTS) as a response to the received RTS, after which the station transmits the packet (DATA) to the AP, and the AP sends an ACK for the DATA received. If a CTS is not received from the AP for the transmitted RTS, the station selects a new BO in the next segment X_{i+1} or CW_e if X_i is the last. The AP transmits an NSP after a point coordination function inter-frame space (PIFS), that is, a period of time after which the transmission channel is considered idle. An idle period, known as a short inter-frame space (SIFS), is used by the receiver during the exchange of frames to mark the end of incoming transmissions. The duration of a PIFS is the sum of an SIFS and a slot time (σ).

Figure 5 shows the flowchart of the steps in STAR, as performed by a station. This scheme is also described as a pseudo-code in Algorithm 1. The AP uses a congestion counter to estimate the size for the next CW_e. The counter is increased by 1 if an RTS is successfully received by the AP or 2 if otherwise. The AP decreases the congestion counter by 1 if it does not receive an RTS for two time slots. The CW_e size for the next CW_e is equal to the current congestion counter, or the default value if the count is smaller than the default value.

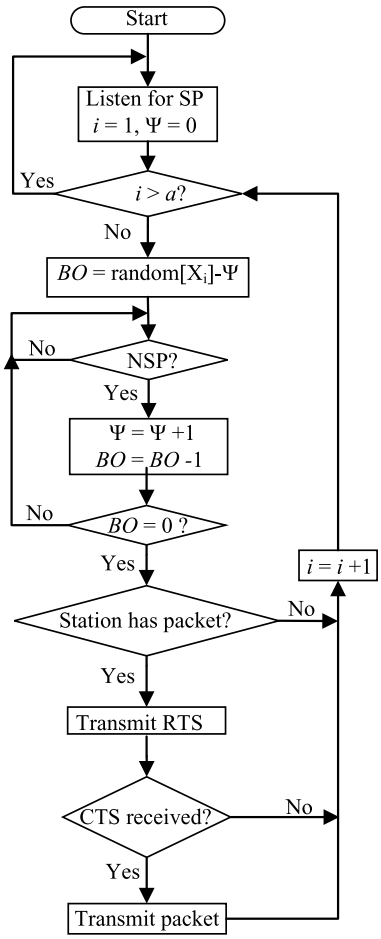

Fig. 5. Flowchart of the steps and processes of STAR.

Algorithm 1. Pseudo-code of the STAR scheme

1: **procedure** Implementing STAR in station s.
2: *listen to the channel for SP*;
3: $a \leftarrow$ *number of the contention attempts*
4: $i = 1$; // i is segment counter
5: $\psi = 0$ // ψ is time slot counter
6: **while** $i \leq a$ **do**
7: $BO \leftarrow random[X_i] - \psi$;
8: **while** $BO > 0$ **do**
9: **if** NSP is received **then**
10: $\psi = \psi + 1$;
11: $BO = BO - 1$;
12: **if** *Station has packet to transmit* **then**
13: *transmit RTS packet*;
14: $i = i + 1$;
15: go to 2;

Algorithm 2 presents the pseudo-code of the algorithm used to estimate the CW_e size.

4. ANALYSIS OF STAR

Figure 6 shows the states and transitions of station s in STAR as a Markov's chain. Let $b(t)$ be the stochastic process that represents the BO count of a given station, P_{id} be the probability that a time slot is idle, and P_{tr} be the probability of at least one transmission in a time slot.

Algorithm 2. Estimate the CW size for the next CW_e

1: $congestion = 0$, $idle\_cnt = 0$, $seq\_ctr = 0$;
2: **if** $congestion \leq 16$ **then**
3: $CW = 16$;
4: $congestion = 16$;
5: **else**
6: $CW = congestion$;
7: $seq\_ctr = 1$, $idle\_ctr = 0$;
8: **while** $seq\_ctr \leq CW$ **do**
9: **if** *AP receives but cannot decode RTS* **then**
10: $congestion = congestion + 2$;
11: **else if** *AP decodes an RTS* **then**
12: $congestion = congestion + 1$;
13: **else if** *AP does not receive an RTS* **then**
14: $idle\_ctr = idle\_ctr + 1$;
15: **if** $(idle\_ctr \bmod 2 = 0)$ **then**
16: $congestion = congestion - 1$;
17: $seq\_ctr = seq\_ctr + 1$.

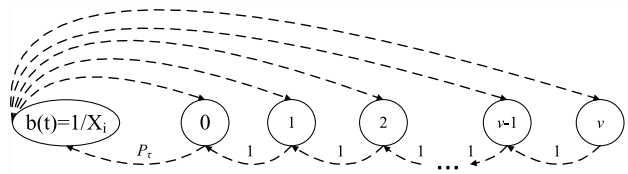

Fig. 6. Markov's chain represents the state transition of a station in STAR.

In general, let

$$b_v = \lim_{t \to \infty} P\{b(t) = v\}$$

be the stationary distribution of the Markov's chain shown in Fig. 6. The BO counter decreases by one count at the beginning of a new time slot. The probability for this change of state is

$$b_{\{v|v+1\}} = 1, \tag{4}$$

because the probability of moving to a new time slot is 1.0; that is,

$$P_{tr} + P_{id} = 1. \tag{5}$$

Let P_τ be the probability that a station's BO state is 0 (i.e., BO = 0); that is,

$$P_\tau = b_0. \tag{6}$$

In a steady state, the following relationships hold:

$$b_{v-1} = b_v, \tag{7}$$

and

$$b_0 = b_v. \tag{8}$$

The BO value is uniformly distributed over X_i. Therefore,

$$b_v = \frac{1}{X_i}. \tag{9}$$

Let c be 1 to 3 for VO, VI, and DA, respectively, and $P_{\mathrm{id},c}$ be the probability that no station transmits a packet of a particular traffic class in a time slot; that is,

$$P_{\mathrm{id},c} = (1 - P_\tau)^{n_c}, \quad 1 \le c \le 3, \tag{10}$$

where n_c is the number of stations that carry the same class of traffic. Therefore, the probability that no packet is transmitted in a time slot is

$$P_{\mathrm{id}} = \prod^{c} P_{\mathrm{id},c}, \tag{11}$$

and the probability that at least one station transmits in a time slot is

$$P_{\mathrm{tr}} = 1 - P_{\mathrm{id}}. \tag{12}$$

The probability that a station successfully transmits a packet of class c traffic ($P_{\mathrm{suc},c}$) occurs when only one station transmits a packet of class c and no station transmits a packet of the other traffic classes on the condition that at least one station transmits a packet [34,35]. This probability is given as

$$P_{\mathrm{suc},c} = n_c P_\tau (1 - P_\tau)^{n_c - 1} \prod^{c'} P_{\mathrm{id},c'} / P_{\mathrm{tr}}, \tag{13}$$

where c' are the traffic classes not transmitted.

The throughput μ of the network is defined as the ratio of the time it takes for a station to transmit only the packet and the time it takes to capture the channel and transmit the packet; that is,

$$\mu = \frac{E[\text{packet duration}]}{E[\text{time taken to transmit the packet}]}$$

or

$$\mu = \frac{P_{\mathrm{tr}} \sum^{c} P_{\mathrm{suc},c} t_{\mathrm{pkt}}}{t_{\mathrm{SP}} + P_{\mathrm{id}} t_{\mathrm{id}} + P_{\mathrm{tr}} \left[\sum^{c} P_{\mathrm{suc},c} t_{\mathrm{suc}} + (1 - \sum^{c} P_{\mathrm{suc},c}) t_{\mathrm{col}} \right]}, \tag{14}$$

where t_{pkt} is the duration of a packet for a given traffic class. t_{id}, t_{suc}, and t_{col} are the duration of an idle, successful, and collision slot, respectively.

Here, t_{id}, t_{col}, and t_{suc} are

$$t_{\mathrm{id}} = t_{\mathrm{NSP}} + t_\sigma, \quad t_{\mathrm{col}} = t_{\mathrm{NSP}} + t_{\mathrm{RTS}} + t_{\mathrm{PIFS}},$$

and

$$t_{\mathrm{suc}} = t_{\mathrm{NSP}} + t_{\mathrm{RTS}} + t_{\mathrm{SIFS}} + t_{\mathrm{CTS}} + t_{\mathrm{SIFS}} + t_{\mathrm{pkt}} + t_{\mathrm{SIFS}} + t_{\mathrm{ACK}} + t_{\mathrm{PIFS}},$$

as shown in Fig. 4(d).

5. PERFORMANCE EVALUATION

We evaluate the performance of STAR through computer simulation and compare its throughput with that theoretically obtained. We also evaluate the throughput and transmission ratio of STAR through computer simulation for different allowed numbers of attempts. Here, we consider three different allowed numbers of attempts where the order of contention attempts is {3,2,1} in the first, {4,2,1} in the second, and {6,3,1} in the third SP. The number of allowed attempts increases for VO and VI in each SP, so that the stations that carry higher priority classes of traffic get assigned more attempts than the stations that carry lower priority traffic. The effect of the increase in the number of allowed attempts is then evaluated. The graphs for the SPs are labeled STAR_1, STAR_2, and STAR_3, respectively. Each simulation is run for 600 s with $n = \{30, 60, ..., 300\}$ and with increasing steps of 30 stations. In the network, a third of the total number of stations carries voice, video, and data traffic. In this simulation, a station always has a packet to transmit. Table 3 summarizes the parameters used for the simulations presented in this paper, unless otherwise stated. Inter-frame spaces (IFSs) in wireless communications, such as in RF communications have been calculated based on the propagation delay, clear channel assessment time, receiver transmitter turnaround time, MAC processing delay, physical layer convergence protocol delay, and the receiver delay for the method of transmission. Such parameters have been studied and standardized to allow communications between devices on a broadcast channel. However, IFSs in NLoS-FSOC are yet to be standardized. Therefore, we employ the parameter values used in IEEE 802.11 standards in our computations. This allows us to evaluate the performance of the system with known IFSs. However, because optical communications can achieve higher transmission speeds than RF communications, we may be able to accommodate much shorter IFSs in NLoS-FSOC.

Table 3. Parameters and the Corresponding Values Used in the Simulation

Parameter	Value (μs)
t_σ	9
t_{PIFS}	16
t_{SIFS}	16
t_{ACK}	20
t_{CTS}	20
t_{RTS}	40
t_{VO}	500
t_{VI}	1000
t_{DA}	2000
t_{SP}	12
t_{NSP}	2

Figure 7(a) shows the throughput for different numbers of attempts and the theoretical throughput. As the figure shows, the throughput decreases as the total number of contention attempts in CW_e increases (i.e., $a_{\mathrm{tot}} = a_{\mathrm{VO}} + a_{\mathrm{VI}} + a_{\mathrm{DA}}$), so that STAR_1 achieves the largest throughput and STAR_3 achieves the smallest throughput. A CW_e with a larger a_{tot} provides more contention opportunities for the competing stations as compared to that of a CW_e with a smaller a_{tot}. However, an increase in the number of contentions also increases the number of collisions in the CW_e, and in turn, it decreases the network throughput. The theoretical throughput in Eq. (14) is evaluated using the average of the last 100 CW_e sizes, as obtained from the simulation. The difference between the theoretical and simulated throughput is $\cong 0.001$, which shows that the theoretical throughput is consistent with the simulated throughput.

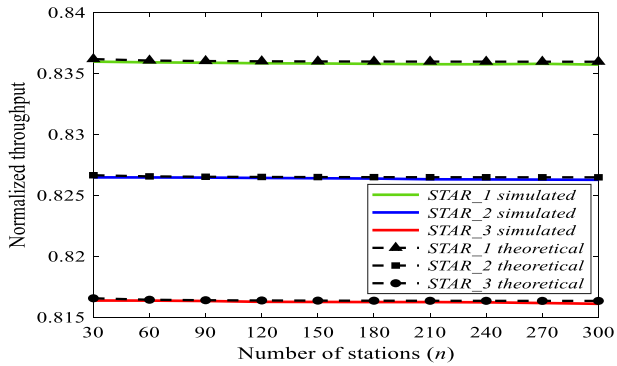

(a)

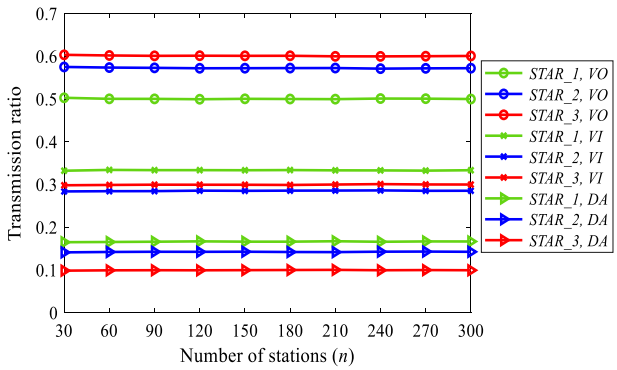

(b)

Fig. 7. Graph of the throughput and transmission ratio in STAR for contention attempts in an SP. (a) Throughput for different lists of contention attempts. (b) Transmission ratio for different lists of contention attempts.

The number of transmitted packets for a class of traffic with a higher priority in the network is expected to be larger than that of a class of traffic with a lower priority for a MAC scheme that handles different traffic classes. Therefore, a comparison of the fraction of transmitted packets for each traffic class shows that the increase in contention opportunities given to the stations with higher priority class of traffic results in an increase in packet transmissions for those traffic classes. The transmission ratio (T) is defined as

$$T = \frac{\text{Number of transmitted packets for a class of traffic}}{\text{Total number of transmitted packets}}$$

or

$$T = \frac{\sum_1^{n_c} N_{c,s}}{\sum_1^{c} \sum_1^{n_c} N_{c,s}}, \tag{15}$$

where $N_{c,s}$ is the total number of packets transmitted by station s for class c. Figure 7(b) shows that more voice packets than video packets are transmitted because voice traffic has a higher priority than video traffic. Likewise, more video packets are transmitted than data packets. The graph shows that STAR_3 achieves the highest transmission ratio of voice packets among those tested because of the ratio of voice attempts in a CW_e, that is, the number of allowed attempts for VO traffic to the total number of allowed attempts. Thus, the transmission ratio is directly correlated to the ratio of attempts for the class of traffic. Likewise, STAR_1 achieves the highest transmission of video and data packets because of the ratio of attempts in the CW_e.

A. Performance Comparison with other Schemes

We compare the performance of STAR with IEEE 802.11, QCAAAE, and STREAM. We selected these schemes because IEEE 802.11 is extensively deployed and QCAAAE and STREAM consider the presence of stations in the network in their contention windows, different traffic classes, and the use of contention for attempting a transmission. However, because these schemes are carrier-sense MAC schemes and because of the void in OLAN-based schemes, we modified them to operate in an OLAN. We compare these schemes by observing the differences in their throughput, energy consumption, transmission ratio, delay, and fairness. Like in STAR, channel access in STREAM and QCAAAE depends on the broadcast information transmitted by the AP in the selection of the BO. A brief description of the implementation of IEEE 802.11, QCAAAE, and STREAM for the optical channel is given as follows:

(i) IEEE 802.11 implements access control for different classes of traffic by combining the arbitration inter-frame spacing (AIFS) and the CW size in the selection of the BO. Here a station chooses a CW size and AIFS number (AIFSN) that corresponds to the class of traffic it carries. IEEE 802.11 uses a binary exponential backoff; that is, for every contention that results in a collision, the station doubles its CW size until the maximum contention window ($\mathrm{CW}_{\max}$) size is reached. The CW size is set to the minimum contention window ($\mathrm{CW}_{\min}$) size when the station receives a CTS from the AP. The BO in IEEE 802.11 for a station is

$$\mathrm{BO} = \mathrm{random}[0 : 2^f \mathrm{CW} - 1], \tag{16}$$

where f is the number of consecutive collisions and $\mathrm{CW}_{\min} \le \mathrm{CW} \le \mathrm{CW}_{\max}$. A station selects the BO for its class of traffic and regressively counts for every passing time slot until the BO is 0, after which the station contends if the channel is idle for a duration equal to its AIFS. By considering the proposed slot structure, we modify the AIFSN of IEEE 802.11 to reflect the removal of channel sensing before contention by stations carrying different classes of traffic. Table 4 shows the modified parameters for IEEE 802.11 to handle the optical channel. Stations implement the AIFSN by counting consecutive idle time slots equal to the AIFSN before contending for channel access.

(ii) QCAAAE selects the CW size and AIFSN according to the broadcast information by the AP. The CW size and AIFSN in QCAAAE accounts for the number of active stations that transmit each class of traffic. $\mathrm{CW}_{\min}$ and $\mathrm{CW}_{\max}$ in QCAAAE are

$$\begin{aligned} \mathrm{CW}_{\min} &= 2^{\lceil \log_2(n_c/2) \rceil} - 1 \\ &\text{and} \\ \mathrm{CW}_{\max} &= 2^{\lceil \log_2(2n_c) \rceil} - 1. \end{aligned} \tag{17}$$

Table 4. IEEE 802.11 Parameters for Different Traffic Classes

Traffic	CW_{min}	CW_{max}	AIFSN
VO	4	8	0
VI	8	16	0
DA	16	1024	1

In addition, $\text{AIFSN} = 2 + \delta_c$, where δ_c indicates the presence of higher-priority traffic in the network. For instance, the AIFSN for VI is 3 if there is at least one station carrying VO traffic in the network; otherwise, the AIFSN is 2. The AP computes n_c and δ_c for the different classes of traffic during the device (or station) association process in a wireless fidelity (WiFi) system where a new device is authenticated and associated with the AP. Changes in n_c and δ_c for the different classes of traffic are broadcast by the AP as they occur. We make the $\text{AIFSN} = \delta_c$ for the optical channel in our simulations.

(iii) In STREAM, a time slot is divided into $m + 1$ minislots in which a station contends for channel access. A station selects the BO and decreases it by 1 after every passing time slot until the BO reaches 0. Here, the BO is selected randomly as

$$\text{BO} = \text{random}[0 : k'n - 1], \tag{18}$$

where k' is the distribution factor associated with the class of traffic, and n is the number of active stations broadcast by the AP. When the BO equals 0, a station randomly selects a minislot number (j) associated with its traffic class and waits for j idle minislots to pass before contending for the channel. If the station senses contention during the count of j, the station defers transmission and selects a new BO; otherwise, the station transmits an RTS. Here, $0 \le j \le m$ is selected according to the traffic class the stations carry; that is,

$$j = \text{random}[j_c], \tag{19}$$

where j_c is the range of selectable minislots for the traffic class. A minislot in STREAM begins with the transmission of an NSP. Table 5 shows the value of k' and the range of j_c associated with each traffic class. For a single class of traffic j_c is randomly selected from [0:3].

The AP maintains a count of stations whose RTS has been received within a time period. Additionally, STREAM uses a congestion counter that increases n_c by 0.5 for every 2 consecutive collisions and it is decreased by 0.75 for every 2 consecutive idle time slots.

We compare the achievable throughput, energy consumption, transmission ratio, delay, and fairness of STAR_2 to those of IEEE 802.11, QCAAAE, and STREAM. We chose STAR_2 because the ratio of the allowed number of attempts to a_{DA} is the same when the CW_{min} of the DA in IEEE 802.11 is divided by the CW_{min} for VO, VI, and DA. We refer to STAR_2 simply as STAR in the remainder of this paper.

Table 5. STREAM Parameters for Different Traffic Classes

Traffic	k'	j_c
VO	0.06	[0:1]
VI	0.12	[0:2]
DA	0.24	[2:3]

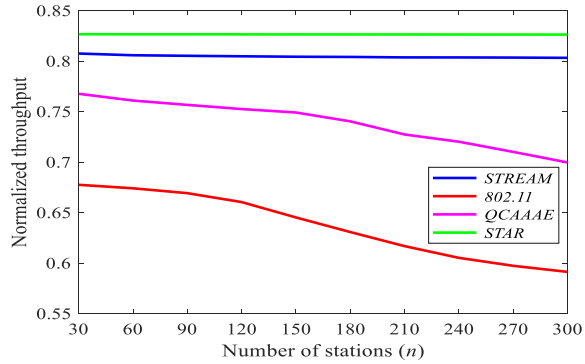

Fig. 8. Throughput of the compared schemes.

1. Throughput Comparison

Figure 8 shows that STAR achieves higher throughput than the compared schemes. The high throughput of STAR is the product of using a large enough CW size for the number of competing stations. Furthermore, the limit on the number of contention attempts in each segment reduces the occurrences of collision as the number of stations in the OLAN grows. Like STAR, STREAM estimates the number of active stations using network events. However, STREAM does not limit the number of contentions for each station. Therefore, the collision rate in STREAM is much higher than that in STAR. As a result, STAR achieves higher throughput than STREAM. The estimated CW size in QCAAAE is small because contending stations experience more collisions and lower throughput than in STAR and STREAM. IEEE 802.11, which is the leading MAC scheme in wireless communications achieves the smallest throughput of 0.675. The throughput of IEEE 802.11 is the lowest among the compared schemes because the CW size in the scheme remains constant despite the growing number of stations in the network. The result is an increase in the number of collisions and a rapid decline in throughput as the number of stations increases. STAR achieves a throughput of 0.825, which is 15% more than that of IEEE 802.11.

Because t_{pkt} for the traffic classes in Table 3 decreases as the priority increases, a scheme that transmits more packets of lower priority may achieve higher throughput than the others. Therefore, we examine the performance for the compared schemes when $t_{pkt} = t_{VO}$ (i.e., $t_{VI} = t_{DA} = t_{VO}$) to show that the throughput performance of the schemes remains the same for the same t_{pkt}. Figure 9 shows the throughput achieved by the compared schemes as the number of stations increases. As expected, the throughput shown in this figure is similar to that in Fig. 8, where STAR performs the best and IEEE 802.11 performs the worst.

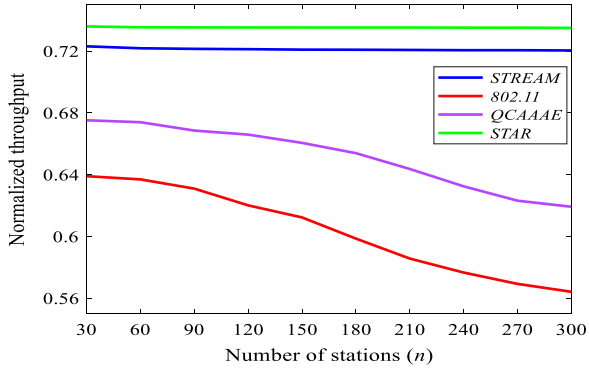

Fig. 9. Throughput when the packet durations are equal for the traffic types.

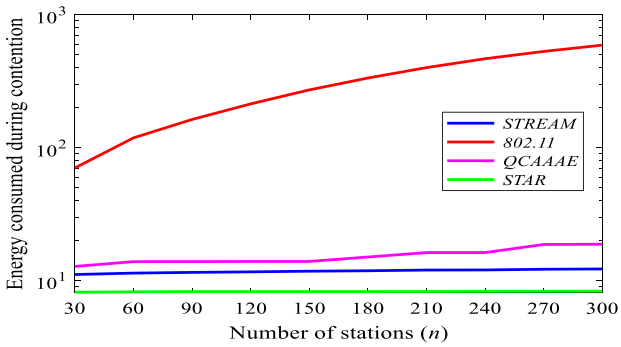

Fig. 10. Energy consumption.

2. Comparison of Energy Consumption

We examine the energy consumption of the compared schemes during contention. We consider only the transmission of RTS because the energy consumed in the receipt of CTS, ACKS, and the transmission of data packets is the same for the compared schemes. Therefore, the total energy consumption (E_c) during contention is also different. E_c is computed as

$$E_c = E_{\mathrm{RTS}} N_{\mathrm{RTS}}, \tag{20}$$

where N_{RTS} is the total number of RTSs, and E_{RTS} is the energy consumed in the transmission of an RTS. We assume that $E_{\mathrm{RTS}} = 20\ \mu\mathrm{J}$ in our analysis.

Figure 10 shows that IEEE 802.11 consumes a large amount of energy because the experienced number of collisions increases as the number of stations also increases. The energy consumption of STAR, STREAM, QCAAAE, and IEEE 802.11 increases to {8.3, 12.2, 18.7, 591.2} J, respectively, for $n = 300$ in the OLAN. STREAM, QCAAAE, and IEEE 802.11 consume about 46%, 120%, and 7000%, respectively, more energy than STAR.

3. Comparison of the Transmission Ratio

Figure 11(a) shows the transmission ratio of the considered schemes for different classes of traffic. It shows that each scheme transmits more packets of higher than of lower priority traffic. IEEE 802.11 does not transmit DA packets as shown in Fig. 11(b) during the simulation period because of

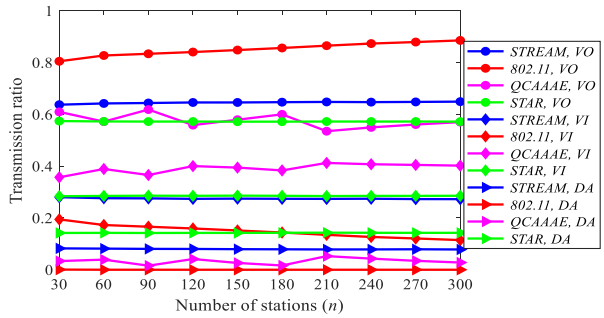

(a)

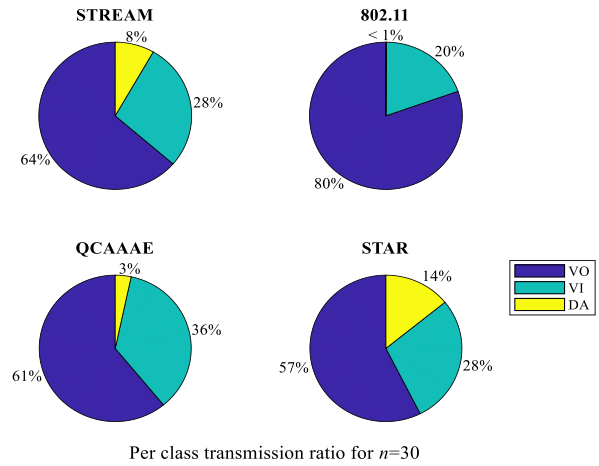

(b)

Fig. 11. Transmission ratio of the compared schemes. (a) Per class transmission ratio. (b) Pie chart of the transmission ratio for $n = 30$.

the implementation of AIFS, and the CW size for DA limits the contention opportunities for stations carrying DA traffic. The CW size for DA traffic in QCAAAE is similar to VO and VI, but it leads to fewer transmissions of DA traffic because of the AIFS implementation. The common values of j_c in STREAM, that is, minislots [0:1] for VO and VI and minislot [2] for VI and DA, allow for the transmission of all the classes of traffic. STAR guarantees contention opportunities for all stations and for each traffic class.

4. Average Delay Comparison

To further examine the impact of the transmission rate of the compared schemes, we examined the average delay of the different traffic classes for each scheme, as shown in Fig. 12. Because each station experiences a different transmission ratio for the classes of traffic, we measure the average delay for each traffic class in the network, where each station transmits 10,000 packets. A station generates a packet randomly every $n * (T_{\mathrm{suc}} + 5\sigma)$ s; that is, the packet generation (G)

$$G = \mathrm{random}[0 : n * (T_{\mathrm{suc}} + 5\sigma)].$$

Figures 12(a)–12(c) show the average delay for VO, VI, and DA traffic, respectively, indicating that the average delay of STAR is the smallest for each traffic class. The delay of the STREAM, QCAAAE, and IEEE 802.11 are larger, in

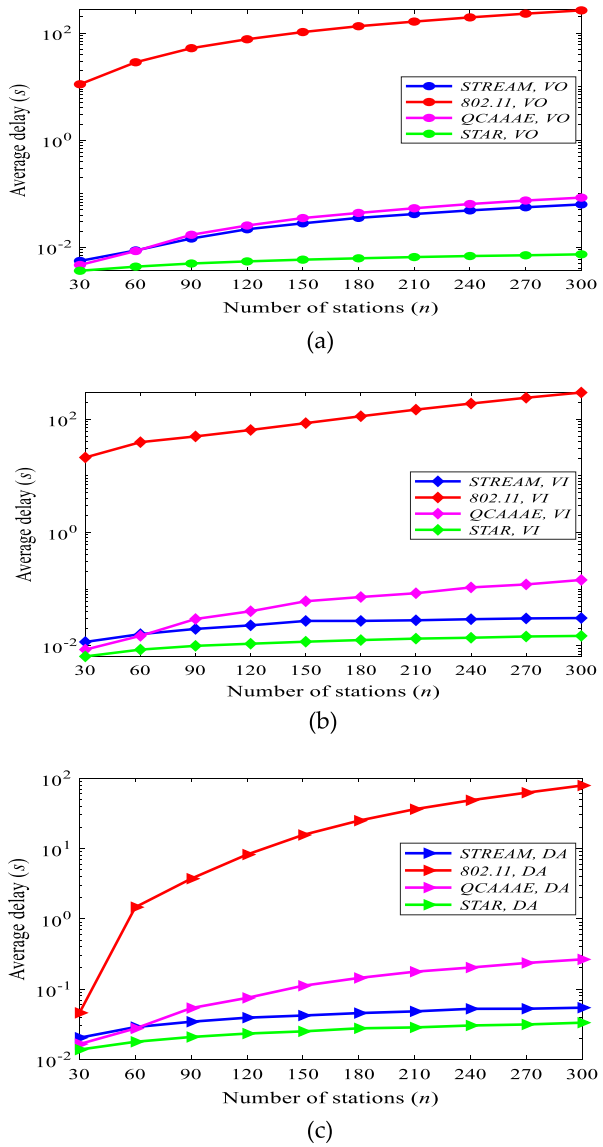

Fig. 12. Average delay for the different traffic classes. (a) Delay for VO traffic only. (b) Delay for VI traffic only. (c) Delay for DA traffic only.

increasing order. The average delay increases as the collision rate experienced by the stations increases. Therefore, the small average delay of STAR is a product of reducing the number of collisions by the CW size. The figure also shows a crossover in the delay of QCAAAE and STREAM as the number of stations increases. The crossover occurs because of the mechanism used in QCAAAE to estimate the CW size and how it produces fewer collisions for a small number of stations, e.g., $n < 60$. The result is a lower delay in QCAAAE than that of STREAM. Compared to the delay performance of STAR, the QCAAAE and STREAM MAC schemes are {0.001,0.002} s slower for VO traffic, {0.002,0.006} s slower for VI traffic, and {0.003,0.007} s slower for DA traffic, respectively, when $n = 30$.

However, IEEE 802.11 experiences the largest number of collisions.

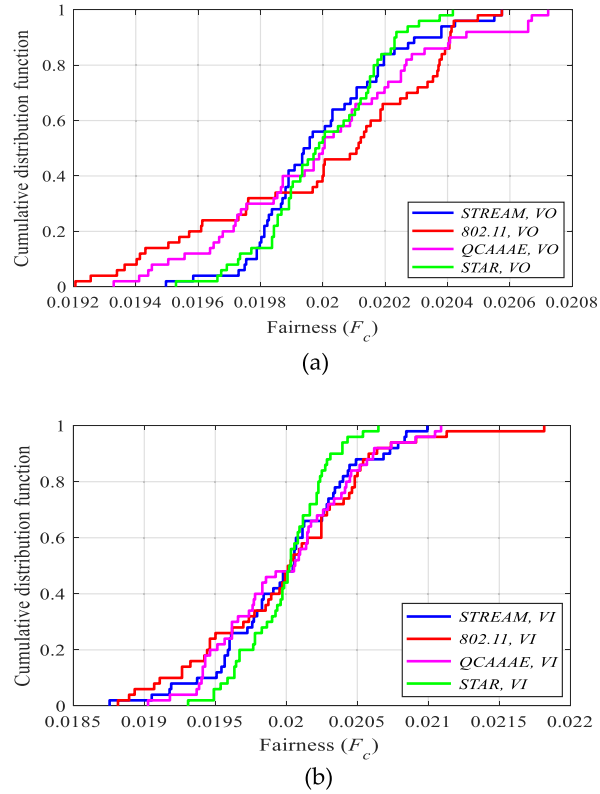

Fig. 13. Fairness for VO and VI traffic. (a) Fairness among stations that carry VO traffic. (b) Fairness among stations that carry VI traffic.

5. Fairness Comparison

We examine the fairness in transmission per traffic class by measuring the contribution of the individual stations to the total number of transmitted packets of each traffic class. That is, for station s that carries traffic class c, the fairness, $F_{c,s}$, experienced by that station is given as

$$F_{c,s} = \frac{N_{c,s}}{\sum_{s=1}^{n_c} N_{c,s}}. \tag{21}$$

We plot the cumulative distributed function of the fairness for VO and VI traffic at $n = 150$ for the compared schemes. When the MAC scheme is fair, stations that carry the same traffic class experience the same contention opportunities and transmit almost the same number of packets. Therefore, the difference in $F_{c,s}$ for the stations carrying the same traffic class is small. A large difference in $F_{c,s}$ implies that some stations experience more contention opportunities than other stations that carry the same traffic class. As a result, the stations with more contention opportunities transmit more packets. As shown in Fig. 13, STAR and IEEE 802.11 achieve the smallest and largest difference in $F_{c,s}$, respectively, as shown for VO traffic in Fig. 13(a) and VI traffic in Fig. 13(b). The limit on the allowed number of contention attempts in a segment for STAR leverages fair access to the transmission channel. Because the CW size and AIFS in both QCAAAE and IEEE 802.11 severely limit the contention opportunities of stations carrying DA traffic, we do not compare the fairness for DA

traffic at $n = 150$ as no packet is transmitted by the end of the simulation for these two schemes.

6. CONCLUSIONS

This paper proposed a time slot structure for nondirect line-of-sight free-space optical communications, or NLoS-FSOC, where an access point uses a broadcast packet, called the new slot packet, to announce the start of a contention slot to the stations in an OLAN. More drastically, our approach rescinds from the conventional use of channel sensing, which is commonly referred to as carrier-sense multiple access with collision avoidance (CSMA/CA). This feature is proposed to work around the features of an NLoS-FSOC OLAN where some stations may not be able to detect the state of the broadcast optical channel, but a proximal access point is able to do so.

We also introduce STAR, a practical MAC scheme based on the proposed time slot structure that achieves sustainable high throughput for different classes of traffic. The discrepancy in the access rates experienced by the stations in STAR is the smallest among all the compared schemes. STAR is based on the principle that the contention window size should be large enough to reduce collisions among a large number of stations in an OLAN. STAR also uses a maximum permissible number of attempts per traffic class to avoid starvation of lower-priority traffic classes.

Our results show that STAR achieves 83% throughput. We also compared the performance of STAR with wireless MAC schemes that were adapted for the optical broadcast channel, such as IEEE 802.11 and other leading MAC schemes, which were originally designed for RF-based wireless networks. In the presented performance comparison, we show that STAR achieves higher performance than the compared schemes. The high performance of STAR is attributed to its dynamic estimation of the contention window size as it provides transmission opportunities for competing stations and reduces the occurrence of collisions.

Acknowledgment. We would like to thank our anonymous reviewers for the constructive and detailed comments that helped us to improve this paper.

REFERENCES

1. Y. Wang, S. Liu, X. Wu, and W. Shi, "CAVBench: a benchmark suite for connected and autonomous vehicles," in *IEEE/ACM Symposium on Edge Computing (SEC)* (2018), pp. 30–42.
2. E. Saini, R. Bhatia, and S. Prakash, "High speed broadband communication system for moving trains using free space optics," in *International Conference on Computational Techniques in Information and Communication Technologies (ICCTICT)* (IEEE, 2016), pp. 47–50.
3. M. Taheri, N. Ansari, J. Feng, R. Rojas-Cessa, and M. Zhou, "Provisioning internet access using FSO in high-speed rail networks," IEEE Netw. **31**, 96–101 (2017).
4. C. Casey, "Free space optical communication in the military environment," Tech. rep. (Naval Postgraduate School, 2014).
5. J. W. Lai, "Free space optical communication for tactical operations," Tech. rep. (Naval Postgraduate School, 2016).
6. A. W. Felder, "Array based free space optic system for tactical communications," Tech. rep. (Naval Postgraduate School, 2018).
7. S. Chaudhary and A. Amphawan, "The role and challenges of free-space optical systems," J. Opt. Commun. **35**, 327–334 (2014).
8. J. Muth, "Building a 'deeper' understanding of underwater optical communications," Laser Focus World **53**, 37–40 (2017).
9. Y. Kaymak, S. Fathi-Kazerooni, and R. Rojas-Cessa, "Indirect diffused light free-space optical communications for vehicular networks," IEEE Commun. Lett. **23**, 814–817 (2019).
10. N. Macaluso, R. Rojas-Cessa, and M. Meo, "Media access schemes for indirect diffused free-space optical networks," in *IEEE 40th Sarnoff Symposium* (IEEE, 2019).
11. P. K. Esubonteng and R. Rojas-Cessa, "Orientation of a diffuse reflector for improved coverage in ID-FSOC for vehicular communications," Veh. Commun. **36**, 100493 (2022).
12. Y. F. Li, P. Yue, and C. He, "Research on radio frequency assignment mechanism of the RoFSO network based on site-specific cognition and utility function," in *Applied Mechanics and Materials* (Trans Tech Publications, 2013), vol. **241**, pp. 2439–2444.
13. S. H. Alnajjar, E. Zuhair S, and F. A. R. Arif, "Performance optimization of hybrid ROFSO link using hybrid optical amplifiers (RAMAN\EDFA) for long-haul transmission with the C-band and L-band comparison," IOP Conf. Ser. Mater. Sci. Eng. **1094**, 012061 (2021).
14. G. Bianchi, "IEEE 802.11-saturation throughput analysis," IEEE Commun. Lett. **2**, 318–320 (1998).
15. H. Wu, S. Cheng, Y. Peng, K. Long, and J. Ma, "IEEE 802.11 distributed coordination function (DCF): analysis and enhancement," in *IEEE International Conference on Communications (ICC)* (IEEE, 2002), vol. **1**, pp. 605–609.
16. M. Heusse, F. Rousseau, R. Guillier, and A. Duda, "Idle sense: an optimal access method for high throughput and fairness in rate diverse wireless LANs," in *Proceedings of the 2005 Conference on Applications, Technologies, Architectures, and Protocols for Computer Communications* (2005), pp. 121–132.
17. T. Li, T. Tang, and C. Chang, "A new backoff algorithm for IEEE 802.11 distributed coordination function," in *Sixth International Conference on Fuzzy Systems and Knowledge Discovery* (IEEE, 2009), vol. **3**, pp. 455–459.
18. Y. Liu, C. Yuen, X. Cao, N. U. Hassan, and J. Chen, "Design of a scalable hybrid MAC protocol for heterogeneous M2M networks," IEEE Internet Things J. **1**, 99–111 (2014).
19. R. A. da Silva, A. Santos, M. Nogueira, K. Boussetta, and N. Achir, "Avoiding collisions by time slot reduction supporting voice and video in 802.11 networks," in *IEEE Global Communications Conference (GLOBECOM)* (IEEE, 2016).
20. Z. Zhao, R. Zhao, J. Xia, X. Lei, D. Li, C. Yuen, and L. Fan, "A novel framework of three-hierarchical offloading optimization for MEC in industrial IoT networks," IEEE Trans. Ind. Inf. **16**, 5424–5434 (2019).
21. S. Kumar, V. S. Raghavan, and J. Deng, "Medium access control protocols for ad hoc wireless networks: a survey," Ad Hoc Netw. **4**, 326–358 (2006).
22. K. Kosek-Szott, "A survey of MAC layer solutions to the hidden node problem in ad-hoc networks," Ad Hoc Netw. **10**, 635–660 (2012).
23. P. K. Esubonteng and R. Rojas-Cessa, "SOSMAC: separated operation states in medium access control for emergency communications on IEEE 802.11-like crowded networks," in *26th Wireless and Optical Communication Conference (WOCC)* (IEEE, 2017).
24. R. Liao, B. Bellalta, M. Oliver, and Z. Niu, "MU-MIMO MAC protocols for wireless local area networks: a survey," IEEE Commun. Surv. Tutorials **18**, 162–183 (2014).
25. IEEE 802 LAN/MAN Standards Committee, "Wireless LAN medium access control (MAC) and physical layer (PHY) specifications," IEEE Standard 802 (1999).
26. N. Abramson, "The ALOHA system: another alternative for computer communications," in *Proceedings of the November 17-19, 1970, Fall Joint Computer Conference* (1970), pp. 281–285.
27. N. Chirdchoo, W.-S. Soh, and K. C. Chua, "Aloha-based MAC protocols with collision avoidance for underwater acoustic networks," in *26th IEEE International Conference on Computer Communications (IEEE INFOCOM)* (IEEE, 2007), pp. 2271–2275.
28. A. Laya, C. Kalalas, F. Vazquez-Gallego, L. Alonso, and J. Alonso-Zarate, "Goodbye, ALOHA!" IEEE Access **4**, 2029–2044 (2016).
29. F. Talucci and M. Gerla, "MACA-BI (MACA by invitation). A wireless MAC protocol for high speed ad hoc networking," in *6th*

International Conference on Universal Personal Communications (ICUPC) (IEEE, 1997), Vol. **2**, pp. 913–917.

30. J. Choi, J. Yoo, S. Choi, and C. Kim, "EBA: an enhancement of the IEEE 802.11 DCF via distributed reservation," IEEE Trans. Mobile Comput. **4**, 378–390 (2005).
31. B. Yang, B. Li, Z. Yan, and M. Yang, "A channel reservation based cooperative multi-channel MAC protocol for the next generation WLAN," Wireless Netw. **24**, 627–646 (2018).
32. M. A. Salem, I. F. Tarrad, M. I. Youssef, A. El-Kader, and M. Sherine, "QoS categories activeness-aware adaptive EDCA algorithm for dense IoT networks," Int. J. Comput. Netw. Commun. **11**, 67–83 (2019).
33. P. K. Esubonteng and R. Rojas-Cessa, "STREAM: medium access control with station presence awareness in crowded networks," IEEE Syst. J. **15**, 5152–5161 (2021).
34. J. R. Gallardo, S. C. Cruz, D. Makrakis, and A. Shami, "Analysis of the EDCA access mechanism for an IEEE 802.11e-compatible wireless LAN," in *IEEE Symposium on Computers and Communications* (IEEE, 2008), pp. 891–898.
35. N. C. Taher, Y. G. Doudane, and B. El Hassan, "A complete and accurate analytical model for 802.11e EDCA under saturation conditions," in *IEEE/ACS International Conference on Computer Systems and Applications* (IEEE, 2009), pp. 800–807.